NASA Technical Memorandum 102677

Integral-Equation Methods in Steady and Unsteady Subsonic, Transonic and Supersonic Aerodynamics For Interdisciplinary Design

E. Carson Yates, Jr.

May 1990

National Aeronautics and Space Administration

Langley Research Center
Hampton, Virginia 23665-5225

Integral-Equation Methods in Steady and Unsteady Subsonic, Transonic and Supersonic Aerodynamics for Interdisciplinary Design

E. Carson Yates, Jr.
Interdisciplinary Research Office, NASA Langley Research Center
Hampton, Virginia, U.S.A.

ABSTRACT

This paper reviews the NASA Langley Research Center program for development of integral-equation aerodynamic methods with emphasis on application in computed-aided multidisciplinary design processes as well as in aerodynamic design and stand-alone analysis. The accomplishments, status, and outlook of the program are discussed in order to highlight the scope, generality, versatility, and attractive features of this methodology.

INTRODUCTION

Progress in the development of computational methods for steady and unsteady aerodynamics has perennially paced advancements in aeroelastic analysis and design capabilities. Since these capabilities are of growing importance in the analysis and design of high-performance aircraft, considerable effort has been directed toward the development of appropriate aerodynamic methodology. This paper reviews the contributions to those efforts from the integral-equations research program at the NASA Langley Research Center. Specifically, the current scope, recent progress, and plans for research and development for inviscid and viscous flows are discussed, and example applications are shown. Although the integral-equations research program was given only limited and intermittent support until about three years ago, it has nevertheless produced some significant results from both in-house and grant-supported work.

INTEGRAL-EQUATION METHODS

The Langley integral-equations program is directed toward general, accurate, efficient, and unified treatment of flows around vehicles having arbitrary shapes, motions, and deformations (including control motions) at subsonic, transonic, and supersonic speeds up to high angles of attack. Special attention is given to real-world design and operating conditions (e.g., Mach number, angle of attack, maneuver) for both fixed-wing and rotor-wing aircraft, as well as to efficient computation for both design and analysis applications. As will be brought out in the subsequent discussion, the integral-equation approach is well suited for these purposes because flow complexities such as viscous effects or transonic flow need to be addressed only in the flow regions where they actually occur, and there is no requirement for patching and matching flow domains or regional solutions. Moreover, for design applications repetitive and nonrepetitive portions of the computations are readily separable, and the required sensitivities of aerodynamic parameters to variations in aircraft geometry can be readily calculated.

Following a long-range plan established a number of years ago, initial efforts addressed the development of surface-panel methods for subsonic [1 to 5] and supersonic [1, 2, 6, 7] linearized potential flow. Current activities include nonlinear methods implementing the full-potential equation for high-subsonic/transonic/low-supersonic speeds [8]. Although the initial high-subsonic/transonic proof-of-concept codes [9 to 11] implemented the small-perturbation potential equation, there is no particular benefit in refining codes for small-perturbation conditions or two-dimensional flow as stepping-stones

toward more realistic conditions. Some computations for two-dimensional flow are made in order to conserve computer resources, however.

In the current program Euler equations are not addressed explicitly. Modification of the full-potential equation to account for entropy changes across shock waves (e.g., as in [12]) should greatly expand the usefulness of potential-flow solutions well into the range of flow conditions that would otherwise require Euler solutions. Consequently, for present purposes we go directly from the modified full-potential method to the Navier-Stokes equations which are being addressed by several investigators with partial support from NASA grants. Methods involving velocity-field decomposition [13 to 16] and direct solution in primitive variables [17, 18] are beings studied. Euler solutions may, of course, be obtained from Navier-Stokes methods with zero viscosity. We are specifically concerned with several types of viscous influences: Thin wakes separating from lifting-surface edges are well represented by inviscid-flow singularities (vortex sheets). Other viscous influences require solution of Navier-Stokes equations or equivalent. These influences include boundary-layer effects, especially on deflected and/or deflecting control surfaces, shock/boundary-layer interaction, and large areas of flow separation in general. Specifics of these problem areas are addressed in the subsequent sections of this paper.

The time-dependent full-potential partial differential equation

$$\nabla^2\phi - \frac{1}{a_\infty^2}\left(\frac{\partial}{\partial t} + U_\infty\frac{\partial}{\partial x}\right)^2\phi = F \tag{1}$$

is the governing equation for most of the work described herein. Application of the generalized Green's-function method to this equation yields an equivalent integral equation for the perturbation velocity potential ϕ at any point P in the flow or on the surface of a body in the flow at any time t [1].

$$\phi(P,t) = \underbrace{\iiint GF\, dV_1\, dt_1}_{\text{nonlinear terms}} + \underbrace{\iiint[\nabla_1 S\cdot(G\nabla_1\phi - \phi\nabla_1 G) - \frac{1}{a_\infty^2}\frac{dS}{dt_1}(G\frac{\partial\phi}{\partial t_1} - \phi\frac{\partial G}{\partial t_1})]\,|\,\square S\,|^{-1}\,dS dt_1}_{\text{linear terms}} \tag{2}$$

where G is the Green's function, F represents all the nonlinear terms, a_∞ is the freestream speed of sound, U_∞ is the freestream speed, x is the coordinate in the freestream direction, $S(x,y,z,t) = 0$ defines the body surface, and

$$|\,\square S\,| = \sqrt{S_x^2 + S_y^2 + S_z^2 + S_t^2}$$

The exact boundary condition on the body surface is

$$\frac{DS}{Dt} = 0 \tag{3}$$

The time integration with respect to t_1 in equation (2) is made trivial by choice of a subsonic or supersonic source pulse as the Green's function.

An important point here is that only the nonlinear terms need to be integrated over a fluid volume. The linear terms are integrated only over the surface of the body and its wake. Note also that the Green's function is a function of freestream Mach number, not local Mach number. Equations (2) and (3) have been formulated and computationally implemented in a moving frame of reference so that they are applicable to problems such as helicopter rotors and maneuvering aircraft as well as aircraft in uniform motion [19 to 23].

Linear Theory

If perturbations from freestream velocity are small, and Mach number is not near one nor too high in the supersonic range, the non-linear terms are negligible, and the

volume integral can be ignored. The remaining surface integral of the linear terms is discretized by surface paneling [2] (e.g., arbitrary twisted quadrilateral panels [3, 4]). The unsteady-flow solution can then be obtained directly by integration in time domain, or a time solution by Laplace transform [2 to 4] converts to complex-frequency-domain form which is generally more efficient for use in solving linear aeroelastic problems.

The velocity potential on the paneled surface is then found in terms of the normalwash distribution which, in general, is known from the input shape, orientation, motion, and deformation.

$$\left[\overset{\approx}{Y}_{jh}\right]\left\{\overset{\approx}{\phi}_{h}\right\} = \left[\overset{\approx}{Z}_{jh}\right]\left\{\overset{\approx}{\Psi}_{h}\right\} \tag{4}$$

where $\overset{\approx}{\phi}_{h}$ is the Laplace transform of the perturbation velocity potential, and $\overset{\approx}{\Psi}_{h}$ is the Laplace transform of the normalwash

$$\overset{\approx}{Y}_{jh} = \delta_{jh} - (C_{jh} + sD_{jh})e^{-s\theta_{jh}} - \sum_{n}(F_{jn} + sG_{jn})S_{nh}e^{-s(\theta_{jn}+\pi_{n})} \tag{5}$$

$$\overset{\approx}{Z}_{jh} = B_{jh}e^{-s\theta_{jh}} \tag{6}$$

δ_{jh} is Kronecker delta, s is the Laplace transform variable (complex frequency), B_{jh}, C_{jh}, D_{jh}, F_{jn}, G_{jn} are integrals over surface panels, Θ_{jh}, π_{jn} are lag functions, and $S_{nh} = \pm 1$ for panels adjacent to a trailing edge on upper or lower surface of the body and is zero otherwise. Surface pressures are obtained from the potential by use of Bernoulli's equation.

Several features of equations (4) to (6) are significant. First, the elements of the Y and Z influence matrices are independent of the normalwash and hence independent of the mode of motion or deflection. Moreover, these matrix elements are simple functions of the complex frequency s so that the cost of changing frequency or calculating for multiple frequencies is small. The influence integrals B, C, and D represent integrals of source, doublet, and "ratelet" distributions over each body-surface panel, and integrals F and G are the corresponding doublet and "ratelet" integrals for wake panels. For a given paneling geometry, all these integrals are functions only of Mach number. If a problem (e.g., dynamic response or flutter) involves multiple modes of normalwash, the normalwash vector in the equation becomes a matrix of modal columns, and the potential distributions for all the modes can be found in a single solution. Similarly, solutions for additional modes or revised modes (as in a structural-design optimization problem) can be obtained without recalculating the Y and Z matrices. For use in design processes, this formulation also appears to provide a general and very efficient means for evaluating sensitivities, i.e., changes in aerodynamic properties caused by changes in external shape [24 to 26].

The generality and versatility of this approach is indicated by its use by Rockwell International for flutter analysis of the space shuttle (fig. 1) in the mid 1970's. Nearly 800 panels were used on the orbiter, and up to 60 modes of motion were used in both symmetric and antisymmetric flutter analyses. Subsequently, the external tank and solid rocket boosters were added, and the calculations were repeated for the entire launch configuration.

For development purposes equations (4) to (6) were implemented in a prototype code called SOUSSA P1.1 (Steady, Oscillatory, and Unsteady Subsonic and Supersonic Aerodynamics - Version 1.1) [3, 4] which is applicable to vehicles having arbitrary shapes, motions, and deformations in subsonic flow only. The P1.1 code employs zeroth-order (constant-potential) panels along with the data base and data-handling utilities of the SPAR finite-element structural-analysis program. These were incorporated because

SOUSSA P1.1 originally was intended for the calculation of steady-state structural loads and unsteady aerodynamics for flutter and gust-response calculation in multidisciplinary structural-optimization computations employing the SPAR structural analysis. The SPAR components, however, are unnecessary for stand-alone use. More efficient data handling methods for stand-alone operation are available.

Subsequent to the completion of SOUSSA P1.1 several significant improvements have been incorporated, and others have been defined [5]. Among the latter are implementation of higher-order panels, elimination of the SPAR components, transposition and revision of the solution algorithm to substantially reduce input/output operations, and improved implementation of the trailing-edge (Kutta) flow condition.

Some program improvements already incorporated in the SOUSSA code include the development of an "out-of-core" solver to permit the use of paneling schemes that lead to coefficient matrices too large to fit in the memory of modest-size computers; the replacement of the paneled wake by an analytical wake (reducing the cost of a typical run by about one-half) but retaining an option to use paneled wakes if needed (e.g., when there is another lifting surface in the wake); and replacing the rectangular integration of pressures by a Gaussian quadrature scheme to improve the accuracy of the calculated generalized aerodynamic forces. These improvements are incorporated in a replacement for the SOUSSA code (generically called UTSA) which is under development at a low level of effort.

Figure 2 (reproduced from [5]) compares a chordwise distribution of pressure coefficient C_p calculated by the SOUSSA surface-panel method with pressures measured on a clipped delta wing oscillating in pitch [27]. The wing had a six-percent-thick circular-arc airfoil. The agreement is good and is representative of results obtained with this code. Figure 3 compares calculated and measured steady upper-surface pressures at two chordwise locations x on an outboard station (y=0.85) on the same clipped delta wing. Two points are to be made: First, in the range of angle of attack α (-2 deg to +2 deg) where pressure varies linearly, the agreement is excellent. Second, for this sharp-edge wing, the influence of the leading-edge vortex is substantial and begins at a low angle of attack. The latter behavior emphasizes the importance of our treatment of vortex-type flow separation to be discussed below. A phenomenological description of the relation between the vortex development and the pressure variation shown is given in [28] (from which figure 3 was taken) and in Appendix A of [27].

In addition to the subsonic capability of the SOUSSA program, a supersonic proof-of-concept surface-panel code has been written to implement linear-theory algorithms developed in [6, 7]. The code employs first-order panels and, like SOUSSA, is applicable to vehicles having arbitrary shapes, motions, and deformations. Initial validations and applications of the code have been conducted.

The only significant difference between subsonic and supersonic formulations is in the expressions for the influence integrals B, C, D, F, G in equations (5) and (6) (see, e.g., [2]). Other portions of the computations, such as basic paneling geometry and solution algorithms are common to both. Consequently, it is possible that the computational capability for supersonic flow derived from this proof-of-concept code will subsequently be incorporated into the subsonic code UTSA.

The status and near-term plans for linear-theory surface-panel methods, which are applicable to vehicles having arbitrary shapes, motions, and deformations, may be summarized as follows: As planned the SOUSSA program will be superseded by an improved program UTSA which incorporates first-order panels as well as other improvements indicated by earlier work with SOUSSA. Ultimately, the code may include both subsonic and supersonic capabilities. Frequency-domain computations are most efficient for implementing linear theory, but a time-domain version is also retained for evaluation

of the surface integral in the nonlinear methods described next. Specific activities include configuring the UTSA code for efficient use in interdisciplinary design processes, incorporating special elements to improve accuracy and efficiency near normalwash discontinuities (e.g., at control surfaces), completing the initial demonstration of the efficient computation of sensitivities of aerodynamic pressures and loads to variations in planform, and general check out and validation.

Nonlinear Theory

When the flow approaches transonic conditions and/or flow perturbations (e.g., angle of attack) become large, the nonlinear terms are no longer negligible, and the volume integral in equation (2) must be evaluated in combination with the surface-panel evaluation of the linear terms [9 to 11]. For nonlinear problems it is important to note (1) that the Green's function depends on freestream Mach number, not local Mach number, and (2) that the integrand of the volume integral diminishes rapidly in magnitude with increasing distance from the body and its wake.

For application to nonlinear problems the integral-equation method has several features which make it particularly attractive for general, efficient computational implementation: (1) Evaluation of an integral is required rather than the numerical solution of a partial differential equation, which is a more sensitive process. (2) The volume integral need be treated only in the limited region of flow in which nonlinear terms are of significant magnitude rather than over an entire computational domain. In fact, as the integration proceeds away from the body, it is terminated when the integrand falls below a preselected threshhold value. (3) Required accuracy can be attained with relatively few computational grid points in the fluid (computational domain of the volume integral). (4) The code is numerically stable even when moderate-to-large time steps are employed. (5) Correct far-field boundary conditions are automatically satisfied. This condition is particularly important for unsteady flow. Linear-theory behavior in the far field is inherent in the integral-equation solution. (6) When viscous flows are treated by velocity-field decomposition (to be discussed below), interfacing (patching and matching) of regional solutions (e.g., inner viscous solution and outer inviscid solution) is not required. (7) Even for solution of nonlinear problems, there is no requirement for generating, imbedding, or interpolating surface-fitted computational grids.

In this section small-perturbation transonic attached flow will be considered first followed by large-perturbation subsonic and transonic flow conditions involving vortex-type flow separation in the form of thin wakes emanating from lifting-surface edges and finally flow conditions involving significant viscous effects which require solution of Navier-Stokes equations for attached or separated flow for which the velocity-field-decomposition method is employed.

Small-Perturbation Transonic Flow For proof-of-concept demonstration of transonic capability, only the small-perturbation terms were retained in the volume integral of equation (2), and the resulting time-domain computer code [11] was called SUSAN (Steady and Unsteady Subsonic Aerodynamics-Nonlinear). Figure 4 shows chordwise pressure distribution near the root of a rectangular wing as calculated by the SUSAN code and by a transonic small-perturbation finite-difference code. The shock is captured, and the agreement is quite good even though only a few elements were used to evaluate the volume integral, and the domain of integration extended only one chord length from the wing perimeter. Good agreement with measured pressures [29] is shown in figure 5 for a sharp-edge wing under conditions involving supercritical flow over much of the chord.

Evolution of lifting pressure ΔC_p on a wing oscillating slowly in pitch about the leading edge is shown in figure 6 at three times during a cycle of motion. Although only ten computational elements along the wing chord were used to evaluate the volume integral of the nonlinear terms, the build-up of lift and the appearance of a shockwave

are clearly indicated. In the figure, symbols are used only to distinguish the curves and do not indicate computational points.

The formulation described here and its implementation in the SUSAN code demonstrated the merits of the integral-equation method for transonic flow. However, no further development of the small-perturbation approximation is planned.

Subsonic/Transonic Flow with Vortex Separation All of the preceding involved calculation of the velocity potential. For solving nonlinear problems, however, there are advantages in calculating velocities directly, especially when large velocity variations occur, when shocks are present, when thin-wake (vortex-like) flow separation from wing leading or side edges occurs (fig. 7), or even when trailing-edge wake deformations are significant. Taking the gradient of the integral equation for the potential (eq. (2)) or alternatively applying the Green's-function method to the full-potential equation in the form (for steady state)

$$\nabla^2\phi = \frac{-1}{\rho}\nabla\rho\cdot\nabla\phi \equiv Q \tag{7}$$

gives [8]

$$\begin{aligned}\bar{V}(x,y,z) = \bar{E}_\infty + \frac{1}{4\pi}\iint_{BODY}\frac{\bar{\omega}\times\bar{R}}{R^3}dS + \frac{1}{4\pi}\iint_{WAKE}\frac{\bar{\omega}\times\bar{R}}{R^3}dS \\ + \frac{1}{4\pi}\iiint_{VOL.}\frac{Q}{R^2}\bar{E}_R dV\end{aligned} \tag{8}$$

where ρ is the fluid density, $\bar{\omega}$ is the vorticity vector, $\bar{R}$ is the vector from "sending" point to "receiving" point, $\bar{E}_R$ is a unit vector in the $\bar{R}$ direction, and $\bar{E}_\infty$ is a unit vector in freestream direction.

Equation (8) is an expression for the velocity field $\bar{V}$ as the sum of four components: (1) freestream, (2) a surface integral which gives the velocity induced by the flow singularities representing the solid body, (3) a surface integral which gives the velocity induced by the vorticity representing the thin wake, and (4) a volume integral representing the compressibility terms (right-hand side of eq. (7)). The integrand of this volume integral decreases more rapidly than the square of the distance from the body or vortex surface, so the domain of integration can be relatively small. The integrands in the three integrals are not independent, and solution is by iteration to satisfy the boundary conditions on the body and to deform the free vortex sheets into a force-free shape [8]. Note that the form of the integrand shown in the body integral indicates the use of a vorticity distribution to represent a thin wing in some proof-of-concept calculations. One of the major generalizations of this method (now in progress) consists of replacing this body integral with the UTSA surface-panel formulation so that transonic flow over bodies of arbitrary shape, including vortex-type separation, can be calculated. Other current improvements include (1) replacing the vortex-lattice model used in the wake integral for proof-of-concept calculations with the hybrid-vortex formulation [30 to 32] in which second-order distributed-vorticity panels are used to compute near-field influence, reducing to zeroth-order (discrete-vorticity) elements for far-field influence, (2) shifting the linear compressibility term $M^2\phi_{xx}$ from volume integral to surface integral by solving

$$\nabla^2\phi - M^2\phi_{xx} = Q - M^2\phi_{xx} \equiv Q_{nonlin} \tag{9}$$

instead of equation (7), thereby significantly reducing the region over which the volume integral needs to be evaluated, (3) replacing constant source strength with linearly varying source strength in the volume elements and introducing a threshold cutoff value for the integrand of the volume integral to terminate integration when the integrand diminishes to negligible magnitude, (4) accelerating convergence of the solution near captured shock waves by possible use of shock fitting [8], (5) accounting for entropy

changes across shockwaves (see, e.g., [12]). Code development for unsteady flow is in progress. Research on suitable configuration of these codes for efficient use in computer-aided interdisciplinary design will be a continuing activity.

Completion of the improvements listed above should provide a powerful tool for calculating transonic and/or free-vortex flows around arbitrary aircraft configurations with sharp leading edges or with specified separation line locations. Establishing the separation line on a vibrating wing, however, is a tough viscous-flow problem, but may be amenable to treatment by the velocity-field-decomposition method to be discussed below. The importance of expediting this activity should be underscored. The ability to calculate accurately the complicated transonic vortical flows around highly swept wings and complete aircraft at high angles of attack is a key problem for the development of highly maneuverable fighter aircraft and is needed to improve the assessment and understanding of steady and transient flight loads and flutter problems of current combat aircraft. It should be especially noted that vortex-type flow separations produce typically detrimental effects on structural loads and flutter.

Figure 8 shows the calculated velocity field and shape of the free-vortex surface in a crossflow plane slightly downstream of the trailing edge of a delta wing with vortex sheets representing thin wakes emanating from leading and trailing edges as in figure 7. The volume integral (eq. (8)) has not been included for this incompressible-flow calculation. The results compare quite favorably with the low-Mach-number experiments of Hummel [33] even though relatively few vortex elements were used in this exploratory calculation. The leading-edge vortex core is clearly defined as is the incipient deformation of the trailing-edge vortex sheet into a trailing-edge core with rotation opposite to that of the leading-edge core. The corresponding spanwise distributions of lifting pressure ΔC_p are shown in figure 9 for crossflow planes at 0.7 and 0.9 of the root chord aft of the wing apex. Agreement with measured values is very good.

Inclusion of the volume integral (eq.(8)) permits calculation of transonic flow. Figure 10 shows the spanwise distribution of upper-surface pressure C_{pu} and the flow field, including a captured shock, in a crossflow plane at 0.8 of the root chord aft of the apex of a delta wing [8]. In this exploratory calculation the vortex sheet was not allowed to roll up enough to exert its full inductive effect on the wing surface before the vorticity was transferred into the vortex core. If an additional quarter turn of rollup were allowed, the pressure peak would be slightly higher and a little farther outboard, resulting in even better agreement with experiment. In contrast, the pressure peak from the Euler solution is considerably weaker and farther outboard than the experimental peak because of spatial and numerical diffusion in the Euler calculation.

Structural design loads do not occur at small-perturbation conditions but at limit load-factor conditions such as high angle of attack. Aeroelastic deformations are important. Wind-tunnel results may be of questionable accuracy because of large wall effects. The important influence of large perturbation conditions and free-vortex flows on structural design loads is typically detrimental, as is illustrated by the calculations shown in figure 11 (from [34]). Even if the linear and nonlinear spanwise load distributions shown were compared on the basis of same total normal force (same area under the curves), it is evident that the effect of the wing-tip vortex is to shift the load outboard and hence increase wing bending moments. Linearized aerodynamic theory indicates that there should be no effect of angle of attack on flutter dynamic pressure. However, a detrimental effect typically does occur with increasing angle of attack (see, e.g., [35 to 37]). If adequate flutter margins are to be maintained when angle of attack is not near zero, the degradation must be predictable. Wind-tunnel testing of stiffness-scaled flutter models is not the answer because they are typically too weak to sustain more than very small static loads. Figure 12 shows experimental variation of flutter dynamic pressure with

angle of attack for a stiff wing that was spring supported [38]. The initial decline in flutter dynamic pressure between 0 and 7 deg is attributed to the effect of the tip vortex. Confirming calculations by methods just described are in early stages. The drastic decline beyond 7 deg is probably caused by flow separation progressing forward from the trailing edge. Prediction of that behavior will require solutions of Navier-Stokes equations as discussed below.

Summarizing the status of integral-equation methods for vortex-type (thin wake) flow separation: The hybrid-vortex method for low-Mach-number steady flow [30 to 32] is complete. Computations based on equation (8) for steady transonic flow with vortex-type separation and shockwaves have been demonstrated [8], and the corresponding unsteady code development is in progress. Major generalizations and improvements in efficiency are underway. Further developments for transonic flow, with or without vortex-type flow separation, will be based on equation (8).

Viscous flow When viscous influences (other than thin wakes from lifting-surface edges) are important—for example, boundary-layer effects on control-surface forces, shock/boundary-layer interaction, or flow separation from surfaces—solution of Navier-Stokes equations in some form is required.

Two approaches have been taken: (a) Potential-vorticity decomposition (PVD) of the velocity-field [13 to 16], and (b) Solution in primitive variables [17, 18].

(a) Potential-vorticity decomposition: The classical Helmholtz representation was considered first. In this approach a vector field (velocity) is expressed as the sum of an irrotational part and a solenoidal part. Thus

$$\bar{v} = \text{grad } \phi + \text{curl } \bar{A} \tag{10}$$

where ϕ is again the scalar potential which is evaluated by the methods already described herein, and the vector potential $\bar{A}$ is related to the vorticity $\bar{\omega}$ by

$$\nabla^2 \bar{A} = -\bar{\omega} = -\text{curl } \bar{v} \tag{11}$$

The vorticity, in turn, is governed by the vorticity-dynamics equation which is obtained by taking the curl of Navier-Stokes equation for general, three-dimensional, unsteady, compresible, viscous, heat-conducting flow [13]. Methods of this type have been used for a long time for viscous incompressible flow, e.g., figs. 13 and 14 (from [14 and 15]), but they have not proved to be readily generalizable to compressible flow.

The problem arises primarily because the vector-potential contribution is solenoidal and has an infinite speed of propagation. Consequently, the essentially irrotational region of the flow contains scalar-potential contributions that are equal and opposite to the vector-potential contribution. Hence, the volume integral must extend over a large region, and the computation becomes costly.

The Poincaré decomposition [16] alleviates this problem because the vortical velocity is obtained by direct integration of the equation which defines vorticity as the curl of the velocity. Hence the vortical velocity is zero over most of the irrotational outer region of the flow, and the computational domain for the volume integral can be comparatively small. This method is being developed further for computational applications.

(b) Solution in primitive variables: The Green's function method has been reformulated to treat vector unsteady and nonlinear equations. The adjoint linear operator has been employed to derive an integral representation of the solution of the Navier-Stokes equations for unsteady three-dimensional compressible flow. Appropriate fundamental solutions for incompresible and compressible flows have been obtained in closed form. These formulations need to be implemented for exploratory computations.

In addition to their value as computational tools, the integral-equation formulations for viscous flows have proved to be very useful for understanding the flow physics such as

relations between boundary conditions, viscous stresses, vorticity generation, convection and diffusion.

Summary of Integral-Equation Activities

The activities described here and the computational capabilities summarized in table I indicate that completion of this work will provide efficient and unified treatment of flow over vehicles having arbitrary shapes, motions, and deformations at subsonic, transonic, and supersonic speeds up to high angles of attack. Moreover, the computational forms of the equations and the computational capabilities that are emerging appear to be well suited for repetitive use in design applications, including calculation of aerodyamic sensitivities, as well as for stand-alone use. As pointed out previously, the UTSA surface-panel program for attached flow may contain both subsonic and supersonic modules in a single program. Flow complexities, such as transonic nonlinearities, thin wakes, or viscous influences, are addressed only if and where they occur. Thus, if the volume-integral module is included with UTSA, the program implements the full-potential equation for transonic nonlinear attached flow. With modification for shock-generated entropy, the program can apply also to flows with shocks of finite strength, including supersonic Mach numbers above the linear range, as long as shock-generated vorticity is of minor importance. If the hybrid-vortex module representing the free vortex sheets is also included, the code treats transonic flow with vortex-type separation. Finally, combination of potential-vorticity decomposition with these scalar-potential methods (PVD formulation) permits the formal equivalent of Navier-Stokes solutions for high angles of attack where flow separation from surfaces may occur (for example, on advanced fighter aircraft in combat maneuvers and in highly transient conditions) and also even for low angles of attack when control-surface deflections or deflection rates are large enough or shock waves are strong enough to cause significant boundary-layer thickening or separation. The latter conditions are particularly important for generating control forces and for design of active control systems.

CONCLUDING REMARKS

Some problems, progress, and plans in the development of steady and unsteady computational aerodynamics for use in aeroelastic analysis and design have been reviewed. The primary focus has been on applications to (1) vehicles having arbitrary shapes, motions, and deformations, (2) appropriate design and operating conditions, especially for transonic speeds and high angles of attack, (3) efficient computation of aerodynamic and aeroelastic behavior for both design and analysis. Current and future activities have been highlighted.

REFERENCES

1. Morino, L. A General Theory of Unsteady Compressible Potential Aerodynamics. NASA CR-2464, 1974.
2. Morino, L. and Chen, L. T. Indicial Compressible Potential Aerodynamics Around Complex Aircraft Configurations. In "Aerodynamic Analysis Requiring Advanced Computers" NASA SP-347, Part II, pp. 1067–1110, 1975.
3. Morino, L. Steady, Oscillatory, and Unsteady Subsonic and Supersonic Aerodynamics—Production Version (SOUSSA P1.1)—Vol. I, Theoretical Manual. NASA CR-159130, 1980.
4. Smolka, S. A.; Preuss, R. D.; Tseng, K.; and Morino, L. Steady, Oscillatory, and Unsteady Subsonic and Supersonic Aerodynamics—Production Version 1.1 (SOUSSA P1.1), Vol. II—User/Programmer Manual. NASA CR 159131, 1980.
5. Yates, E. C., Jr.; Cunningham, H. J.; Desmarais, R. N.; Silva, W. A.; and Drobenko, B. Subsonic Aerodynamic and Flutter Characteristics of Several Wings Calculated by the SOUSSA P1.1 Panel Method. AIAA Paper 82-0727, 1982.

6. Freedman, M. I.; Sipcic, S.; and Tseng, K. A First-Order Green's Function Approach to Supersonic Oscillatory Flow—A Mixed Analytic and Numerical Treatment. NASA CR-172207, 1984.
7. Freedman, M. I.; and Tseng, K. A First-Order Time-Domain Green's Function Approach to Supersonic Unsteady Flow. NASA CR-172208, 1985.
8. Kandil, O. A.; and Yates, E. C., Jr. Computation of Transonic Vortex Flows Past Delta Wings—Integral Equation Approach. AIAA Journal, Vol. 24, No. 11, 1986, pp. 1729–1736.
9. Morino, L.; and Tseng, K. Time-Domain Green's Function Method for Three-Dimensional Nonlinear Subsonic Flows. AIAA Paper 78-1204, 1978.
10. Tseng, K. and Morino, L. Nonlinear Green's Function Method for Unsteady Transonic Flows. In "Transonic Aerodynamics" (Ed. Nixon, D.) AIAA Series, Progress in Aeronautics and Astronautics, Vol. 81, 1982, pp. 565-603.
11. Tseng, K. Nonlinear Green's Function Method for Transonic Potential Flow. Ph.D. Dissertation, Boston University, 1983.
12. Fuglsang, D. F.; and William, M. H. Non-Isentropic Unsteady Transonic Small Disturbance Theory. AIAA Paper 85-0600, 1985.
13. Morino, L. Scalar/Vector Potential Formulation for Compressible Viscous Unsteady Flows. NASA CR-3921, 1985.
14. Morino, L. Helmholtz Decomposition Revisited: Vorticity Generation and Trailing Edge Condition. Part 1: Incompressible Flows. Computational Mechanics, Vol. 1, 1986, pp. 65–90.
15. Morino, L.; Bharadvaj, B. K.; and Del Marco, S. P. Helmholtz Decomposition and Navier-Stokes Equations. In "Proceedings of International Conference on Computational Mechanics", 1986, Tokyo, Japan.
16. Morino, L. Helmholtz and Poincaré Potential-Vorticity Decompositions for the Analysis of Unsteady Compressible Viscous Flows. In "Developments in Boundary Element Methods. Vol. 6: Nonlinear Problems of Fluid Dynamics" (Eds. P. K. Banerjee and L. Morino) Elsevier Applied Science Publishers, Barking, U.K., 1989.
17 Piva, R.; and Morino, L. Vector Green's Function Method for Unsteady Navier-Stokes Equations". Meccanica, Vol. 22, 1987, pp. 76–85.
18. Piva, R.; and Morino, L. A Boundary Integral Formulation in Primitive Variables for Unsteady Viscous Flows. In "Developments in Boundary Element Methods. Vol. 6: Nonlinear Problems of Fluid Dynamics" (Eds. P. K. Banerjee and L. Morino) Elsevier Applied Science Publishers, Barking, U.K., 1989.
19. Soohoo, P.; Noll, R. B.; Morino, L.; and Hamm, N. D. Rotor Wake Effects on Hub/Pylon Flow. Vol. I, Theoretical Formulation. Applied Technology Laboratory, U. S. Army Research and Technology Laboratories (AVRADCOM), Fort Eustis, VA, USARTL-TR-78-1A, 1978, p. 108.
20. Morino, L.; Kaprielian, Z., Jr.; and Sipcic, S. R. Free Wake Analysis of Helicopter Rotors. Vertica, Vol. 9, No. 2, 1985, pp. 127–140.
21. Morino, L.; and Bharadvaj, B. K. Two Methods for Viscous and Inviscid Free-Wake Analysis of Helicopter Rotors. CCAD-TR-85-04-R, Boston University, 1985.
22. Bharadvaj, B. K.; and Morino, L. Free-Wake Analysis of Helicopter Rotors: A Boundary Element Approach. BETECH 86, Proceedings of the 2nd Boundary Element Technology Conference, MIT, USA, pp. 291–303, Computational Mechanics Publications, 1986.
23. Morino, L.; and Tseng, K. A General Theory of Unsteady Compressible Potential Flows With Applications to Airplanes and Rotors. In "Developments in Boundary

Element Methods. Vol. 6: Nonlinear Problems of Fluid Dynamics" (Eds. P. K. Banerjee and L. Morino) Elsevier Applied Science Publishers, Barking, U.K., 1989.

24. Yates, E. C., Jr. Aerodynamic Sensitivities from Subsonic, Sonic, and Supersonic Unsteady, Nonplanar Lifting-Surface Theory. NASA TM 100502, 1987.
25. Yates, E. C., Jr.; and Desmarais, R. N. Calculation of Aerodynamic Sensitivities by Boundary-Integral Methods and Application to Lifting-Surface Theory. Proceedings of the International Symposium on Boundary Element Methods (ISBEM89), East Hartford, CT, 1989. Springer Verlag, New York and Heidelberg, 1990.
26. Yates, E. C. Jr.; and Desmarais, R. N. Boundery-Integral Method for Calculating Aerodynamic Sensitivities with Illustration for Lifting-Surface Theory. Proceedings of the Third International Congress of Fluid Mechanics, Cairo, Egypt, 1990.
27. Hess, R. W.; Cazier, F. W.; and Wynne, E. C. Steady and Unsteady Transonic Pressure Measurements on a Clipped-Delta Wing for Pitching and Control-Surface Oscillations. NASA TP 2594, 1986.
28. Yates, E. C. Jr.; and Olsen, J. J. Aerodynamic Experiments with Oscillating Lifting Surfaces—Review and Preview. AIAA Paper 80-0450. Invited Lecture given at AIAA 11th Aerodynamic Testing Conference, Colorado Springs, 1980.
29. Knechtel, E. D. Experimental Investigation at Transonic Speeds of Pressure Distributions over Wedge and Circular-Arc Airfoil Sections and Evaluation of Perforated Wall Interference. NASA TN D-15, 1959.
30. Kandil, O. A.; Chu, L. C.; and Yates, E. C., Jr. Hybrid Vortex Method for Lifting Surfaces with Free Vortex Flow. AIAA Paper 80-0070, 1980.
31. Kandil, O. A.; Chu, L.; and Turead, T. A Nonlinear Hybrid Vortex Method for Wings at Large Angle of Attack. AIAA Journal, Vol. 22, No. 3, 1984.
32. Chu, L. C.; Yates, E. C., Jr.; and Kandil, O. A. Integral Equation Solution of the Full Potential Equation for Transonic Flows. AIAA Paper 89-0563, 1989.
33. Hummel, D. J. On the Vortex Formation Over a Slender Wing at Large Angles of Incidence. AGARD CP 247, 1978.
34. Kandil, O. A. Prediction of the Steady Aerodynamic Loads on Lifting Surfaces Having Sharp-Edge Separation. Ph.D. Dissertation, Virginia Polytechnic Institute and State University, 1974.
35. Houwink, R.; Kraan, A. N.; and Zwaan, R. J. Wind-Tunnel Study of the Flutter Characteristics of a Supercritical Wing. Journal of Aircraft, Vol. 19, No. 5, 1982, pp. 400–405.
36. Yates, E. C., Jr.; Wynne, E. C.; Farmer, M. G. Effects of Angle of Attack on Transonic Flutter of a Supercritical Wing. Journal of Aircraft, Vol. 20, No. 10, 1983, pp. 841–847.
37. Yates, E. C., Jr.; and Chu, L. C. Static Aeroelastic Effects on the Flutter of a Supercritical Wing. In "Static Aeroelastic Effects on High Performance Aircraft", AGARD CP No. 403, 1986.
38. Farmer, M. G. A Two-Degree-of-Freedom Flutter Mount System with Low Damping for Testing Rigid Wings at Different Angles of Attack. NASA TM 83302, 1982.
39. Howarth, L. On the Solution of the Laminar Boundary Layer Equations. Proceedings of the Royal Society A, London, 1938, p. 164.

Table 1.-Summary of Integral-Equation Activities.

α Range \ M Range	Subsonic	Transonic	Supersonic
Low (attached flow) w/large control deflection	UTSA PVD	Nonlinear UTSA PVD	UTSA
Moderate (vortex separation) w/large control deflection	UTSA + Hybrid vortex PVD	Nonlinear UTSA + Hybrid vortex PVD	
Large (separated flow) w/ or w/o control deflection	PVD PVD	PVD PVD	

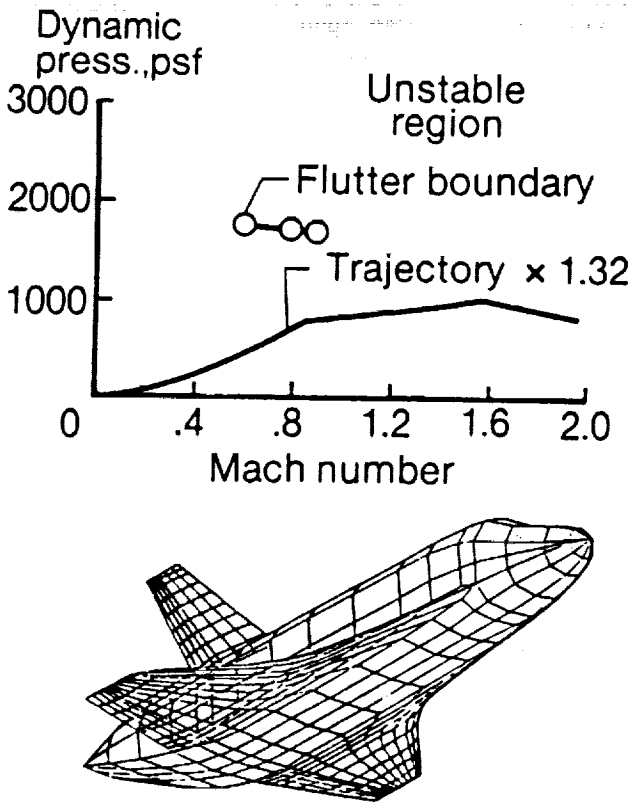

Fig. 1-Shuttle orbiter flutter analysis

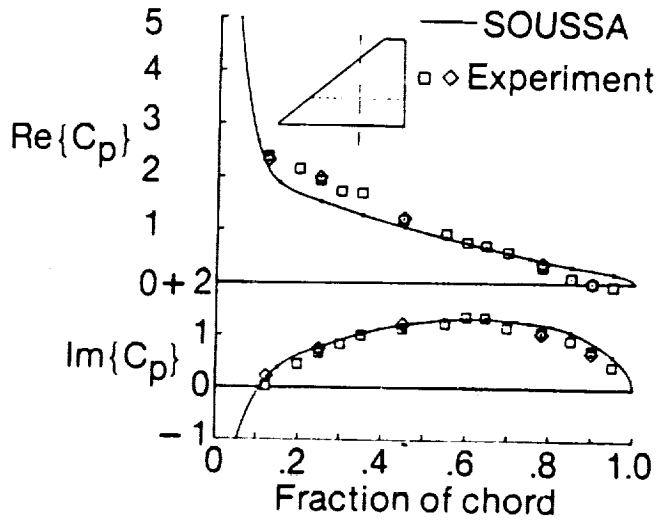

Fig. 2-Unsteady surface pressures on clipped-delta wing at Mach number 0.4, reduced frequency 0.66

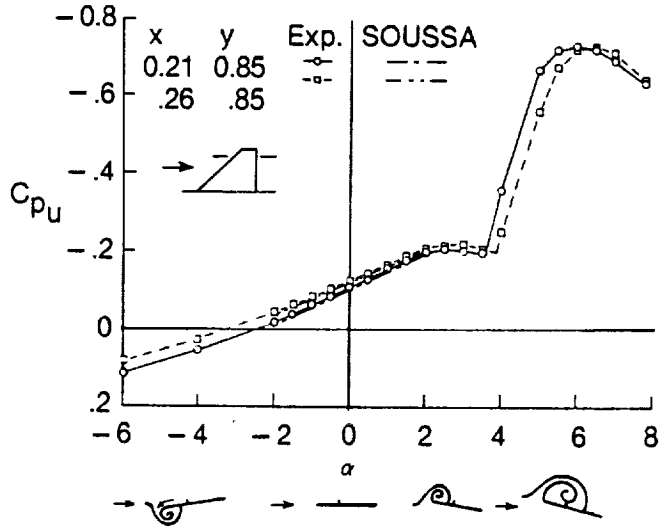

Fig. 3-Steady pressures on clipped-delta wing with 6-percent biconvex airfoil at Mach number 0.4, Reynolds number $2.x10^6$

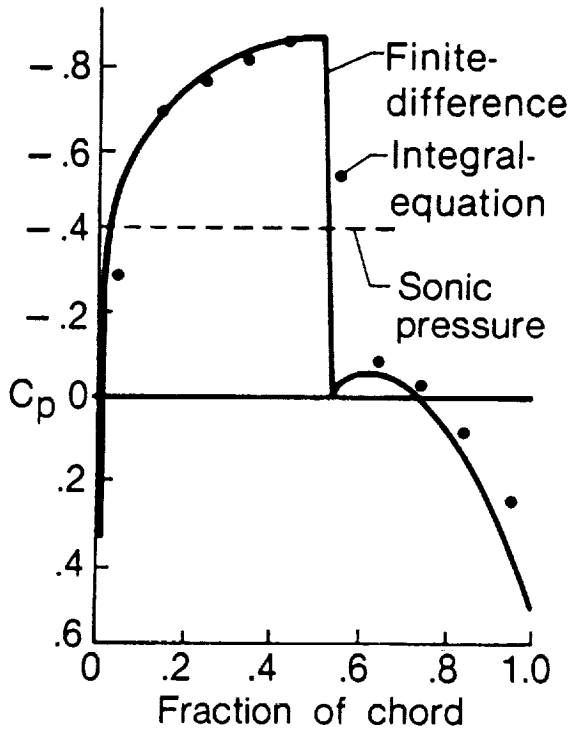

Fig. 4-Steady pressures near root of aspect-ratio 6 rectangular wing with NACA 0012 airfoil at Mach number 0.82, α=0

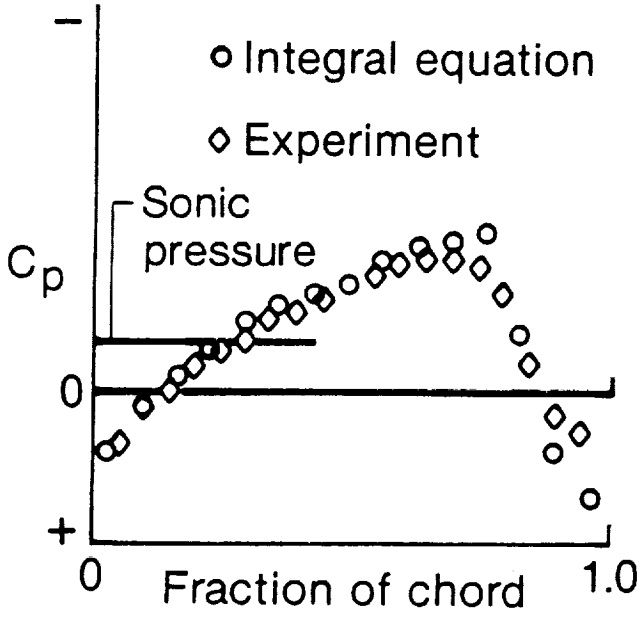

Fig. 5-Steady pressures for aspect-ratio 4 rectangular wing with 6% biconvex airfoil at Mach number 0.908, α=0

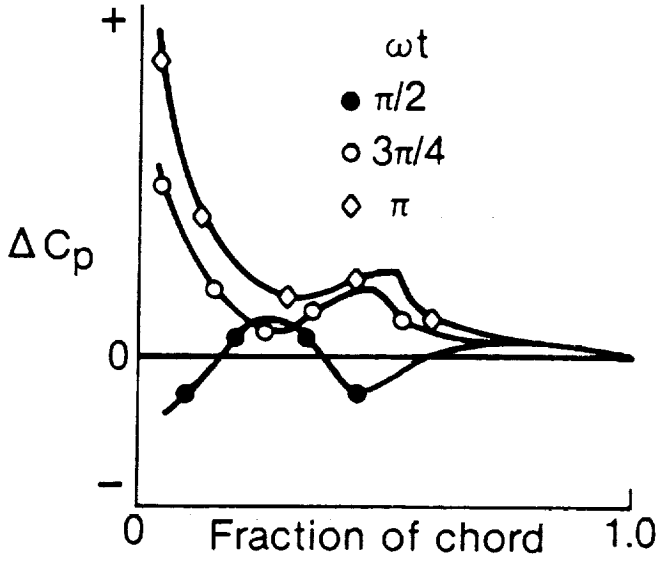

Fig. 6-Unsteady pressures for aspect-ratio 5 rectangular wing with NACA 64A006 airfoil pitching at reduced frequency 0.06, Mach number 0.875

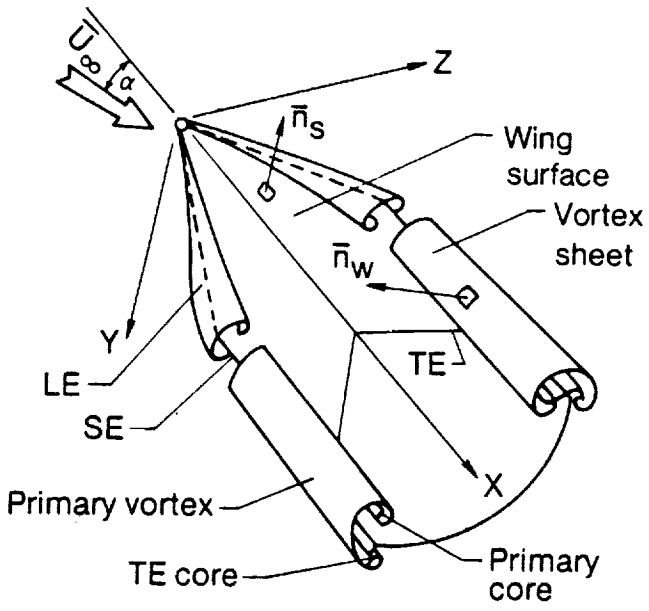

Fig. 7-Sketch of vortex sheets separating from wing edges

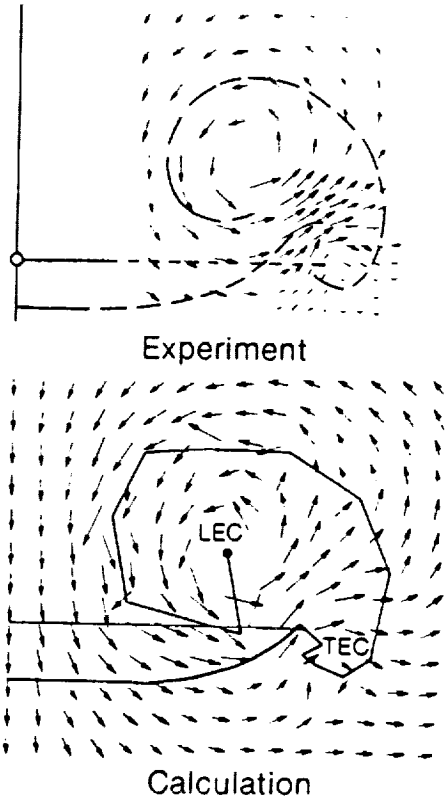

Fig. 8-Flow field behind aspect-ratio 1 delta wing at $\alpha=20.5^o$

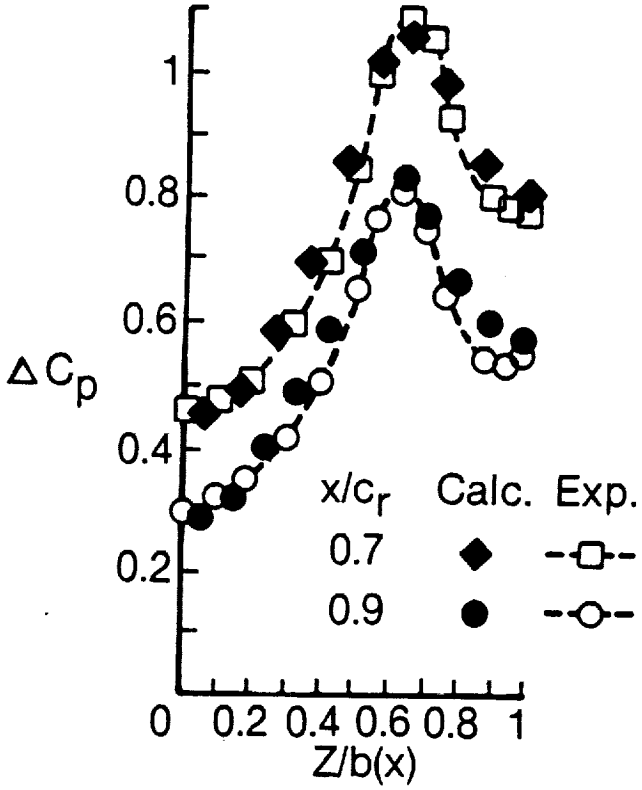

Fig. 9-Steady pressures on aspect-ratio 1 delta wing at $\alpha=20.5^o$

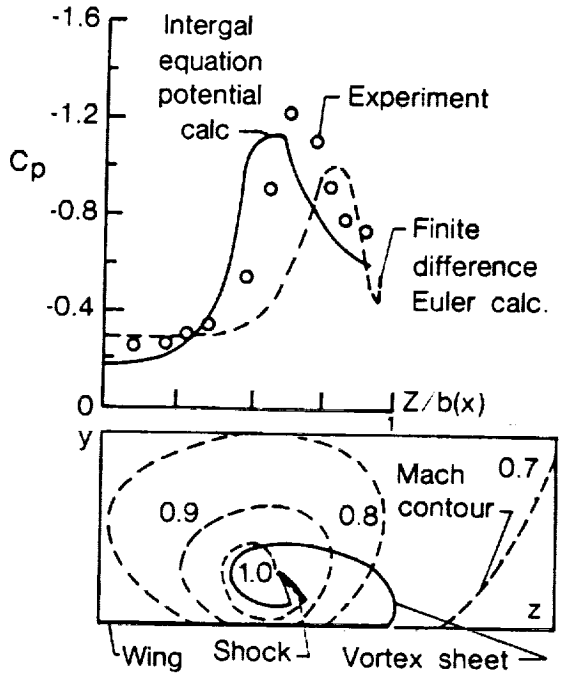

Fig. 10-Steady pressures on aspect-ratio 1.5 delta wing at Mach number 0.7, $\alpha=15.^o$, $x/c_r=0.8$

NASA
National Aeronautics and Space Administration

Report Documentation Page

1. Report No.	2. Government Accession No.	3. Recipient's Catalog No.
NASA TM-102677		

4. Title and Subtitle	5. Report Date
Integral-Equation Methods in Steady and Unsteady Subsonic, Transonic and Supersonic Aerodynamics for Interdisciplinary Design	May 1990
	6. Performing Organization Code

7. Author(s)	8. Performing Organization Report No.
E. Carson Yates, Jr.	
	10. Work Unit No.
	505-63-01

9. Performing Organization Name and Address	11. Contract or Grant No.
NASA Langley Research Center Hampton, VA 23665-5225	
	13. Type of Report and Period Covered
12. Sponsoring Agency Name and Address	Technical Memorandum
National Aeronautics and Space Administration Washington, DC 20546-0001	14. Sponsoring Agency Code

15. Supplementary Notes

Invited paper presented at Japan/USA Boundary Elements Symposium, Palo Alto, CA, 5-7 June 1990.

16. Abstract

Progress in the development of computational methods for steady and unsteady aerodynamics has perennially paced advancements in aeroelastic analysis and design capabilities. Since these capabilities are of growing importance in the analysis and design of high-performance aircraft, considerable effort has been directed toward the development of appropriate aerodynamic methodology. This paper reviews the contributions to those efforts from the integral-equations research program at the NASA Langley Research Center. Specifically, the current scope, progress, and plans for research and development for inviscid and viscous flows are discussed, and example applications are shown in order to highlight the generality, versatility, and attractive features of this methodology.

17. Key Words (Suggested by Author(s))	18. Distribution Statement
Nonlinear Aerodynamics Unsteady Aerodynamics Transonic Aerodynamics	Unclassified - Unlimited Subject Category - 02

19. Security Classif. (of this report)	20. Security Classif. (of this page)	21. No. of pages	22. Price
Unclassified	Unclassified	16	A03

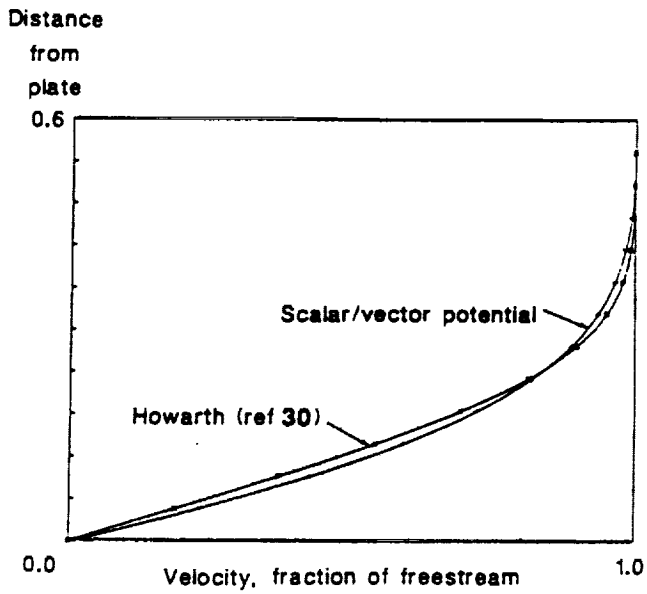

Fig. 13- Velocity in laminar boundary layer on a flat plate in incompressible flow

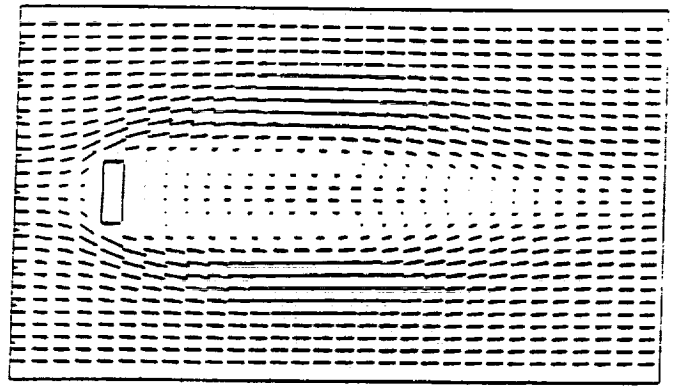

Fig. 14- Velocity field around a rectangle in incompressible flow

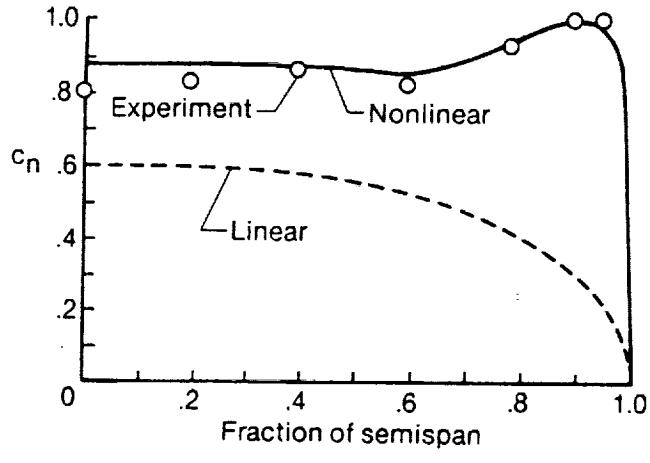

Fig. 11-Steady spanwise variation of local normal-force coefficient for aspect-ratio 1 rectangular wing at α=19.4°

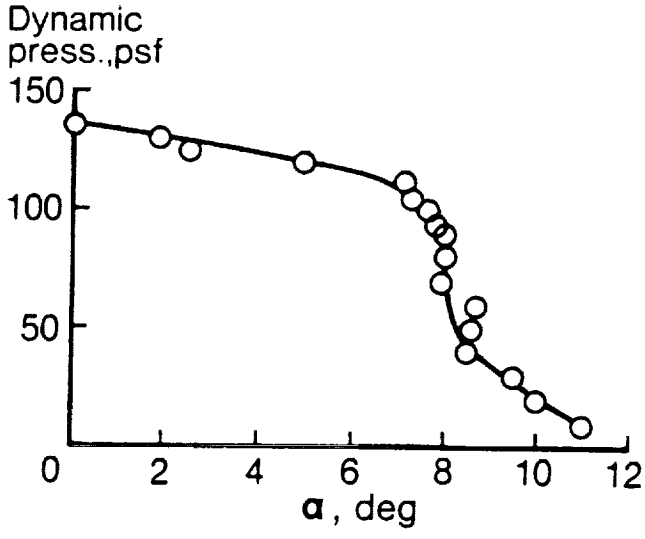

Fig. 12-Effect of angle of attack on flutter of aspect-ratio-6 rectangular wing with NACA 64A010 airfoil